Supporting Information

Design Considerations of Iron-Based Nanoclusters for Non-Invasive Tracking of Mesenchymal Stem Cell Homing

Xinglu Huang, [†§] Fan Zhang, [†‡§] Yu Wang, [†] Xiaolian Sun, [†] Ki Young Choi, [†] Dingbin Liu, [†] Jin-sil Choi,[¶] Tae-Hyun Shin,[¶] Jinwoo Cheon,[¶] Gang Niu,[†] Xiaoyuan Chen[†]*

[†]Laboratory of Molecular Imaging and Nanomedicine (LOMIN), National Institute of Biomedical Imaging and Bioengineering (NIBIB), National Institutes of Health (NIH), Bethesda, Maryland, 20892, USA

[‡] Center for Molecular Imaging and Translational Medicine, School of Public Health, Xiamen University (China)

[¶]Department of Chemistry, Yonsei University, Seoul, 120-749, Korea

*Corresponding Author: e-mail; Shawn.Chen@nih.gov

[§]These authors contributed equally to this work.

RECEIVED DATE (to be automatically inserted after your manuscript is accepted if required according to the journal that you are submitting your paper to)

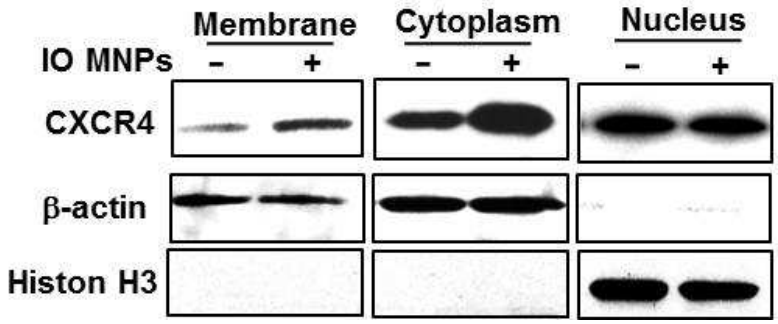

Figure S1. Western blot analysis of CXCR4 expression in different subcellular protein fractions after IO MNP treatment.

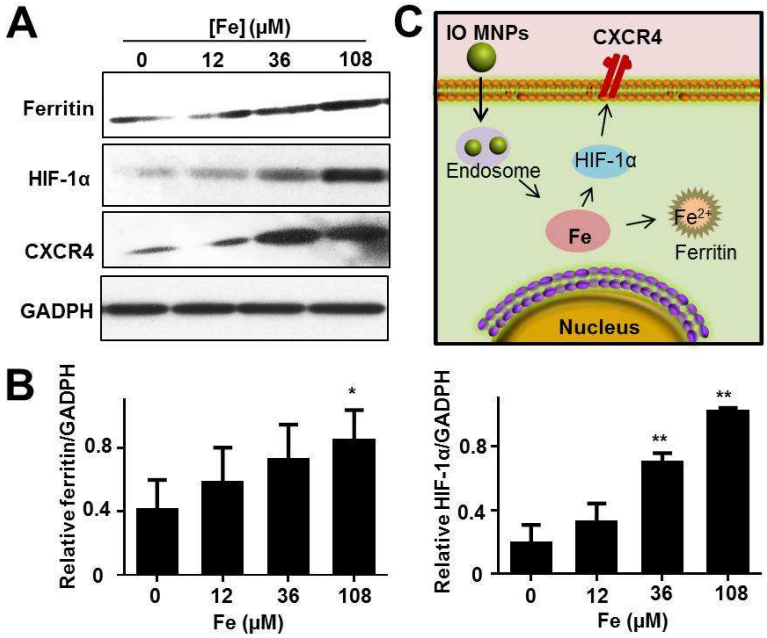

Figure S2. Potential mechanism of increased CXCR4 expression by iron-based MNPs treatment. (A) Western blot analysis of the protein expression of CXCR4, HIF-1α and ferritin after treatment with different iron concentrations. (B) Quantification analysis of CXCR4, HIF-1α and ferritin expression (*$p < 0.05$, **$p < 0.01$). (C) Schematic depiction of potential mechanism of

enhanced CXCR4 expression by IO MNPs. After uptake of IO MNPs, HIF-1α expression of MSCs is increased by releasing iron ions, and further regulates CXCR4 expression.

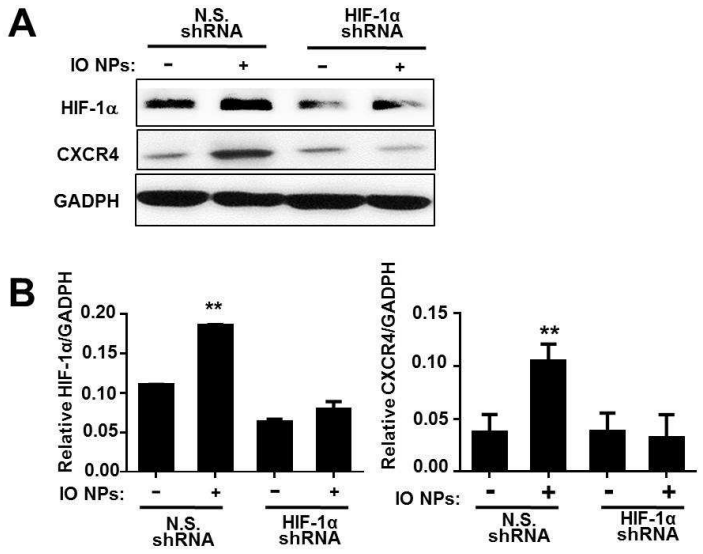

Figure S3. HIF-1α mediated iron-based MNPs upregulated CXCR4 expression. (A) MSCs were transduced with lentivirus containing HIF-1α shRNA, and then treated with IO MNPs. (B) HIF-1α and CXCR4 expression levels were quantified by western blotting (**$p < 0.01$).

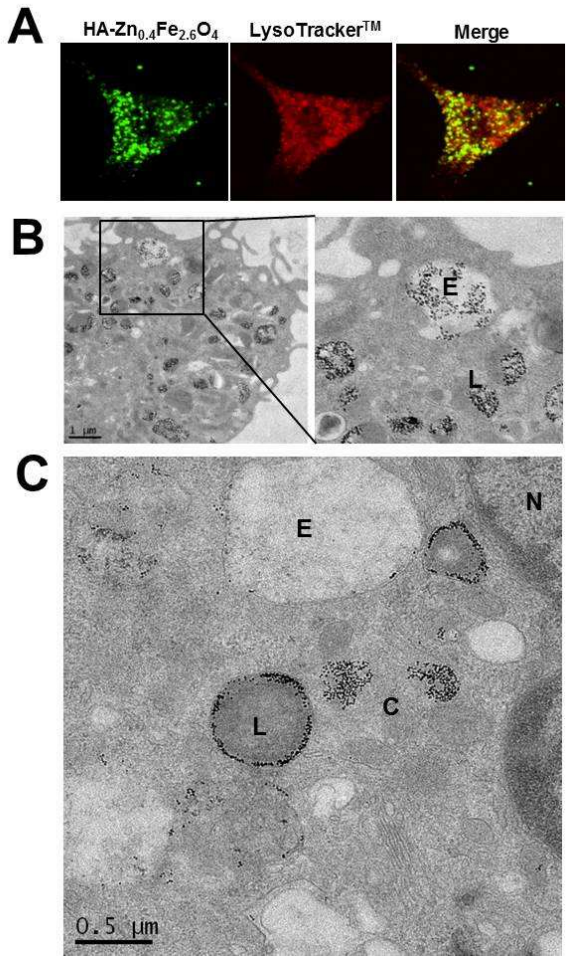

Figure S4. Intracellular localization of HA-$Zn_{0.4}Fe_{2.6}O_4$ NC. The MSCs were incubated with the NC for 2 h. (A, B) The NC intracellular distribution was illustrated by co-localization of the particles and endosome in confocal microscope (A) and TEM images (B). (C) The localization of HA-$Zn_{0.4}Fe_{2.6}O_4$ NC was also performed 24 h after labeling. TEM image illustrated that a portion of the particles escaped from the lysosome and released into the cytosol of MSCs. E: endosome; L: lysosome; C: cytoplasm; N: nucleus.

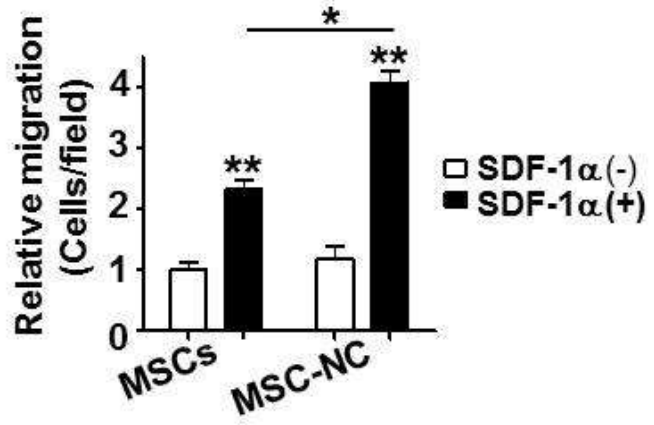

Figure S5. Migration capacity of MSCs untreated and treated with HA-$Zn_{0.4}Fe_{2.6}O_4$ NC in the presence and absence of SDF-1α. (* $p < 0.05$, ** $p < 0.01$)

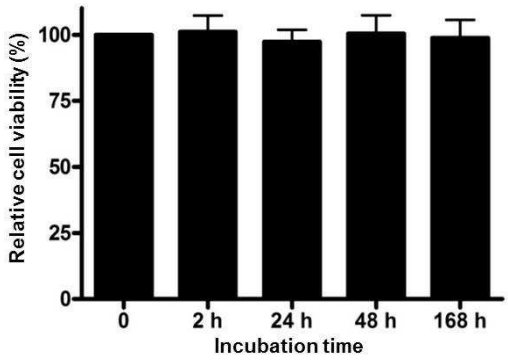

Figure S6. After treatment with 108 μM NC at different time points, *in vitro* cytotoxicity was investigated by standard MTT assay, showing no obvious change in cell proliferation after labeling.

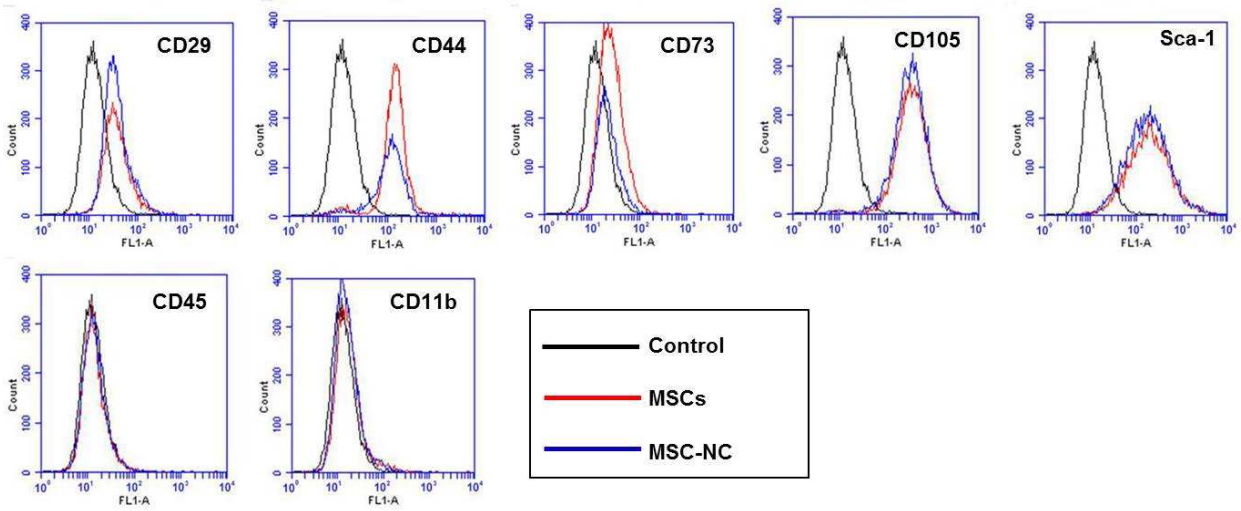

Figure S7. FACS analyses of the surface markers of unlabeled and labeled MSCs after 10 days treatment.

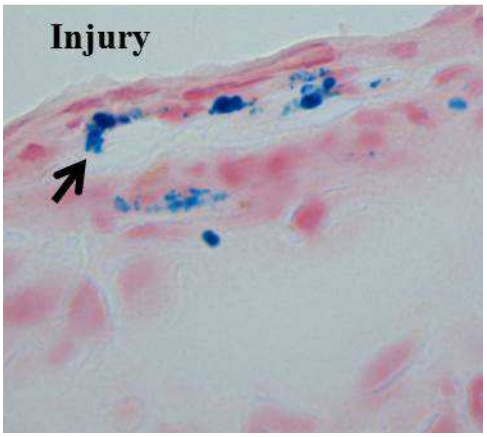

Figure S8. Prussian blue staining of targeted delivery of HA-$Zn_{0.4}Fe_{2.6}O_4$ NC-labeled MSCs to TBI (arrow). At 48 h post-injection, the mice were sacrificed and frozen tissue slices were prepared.

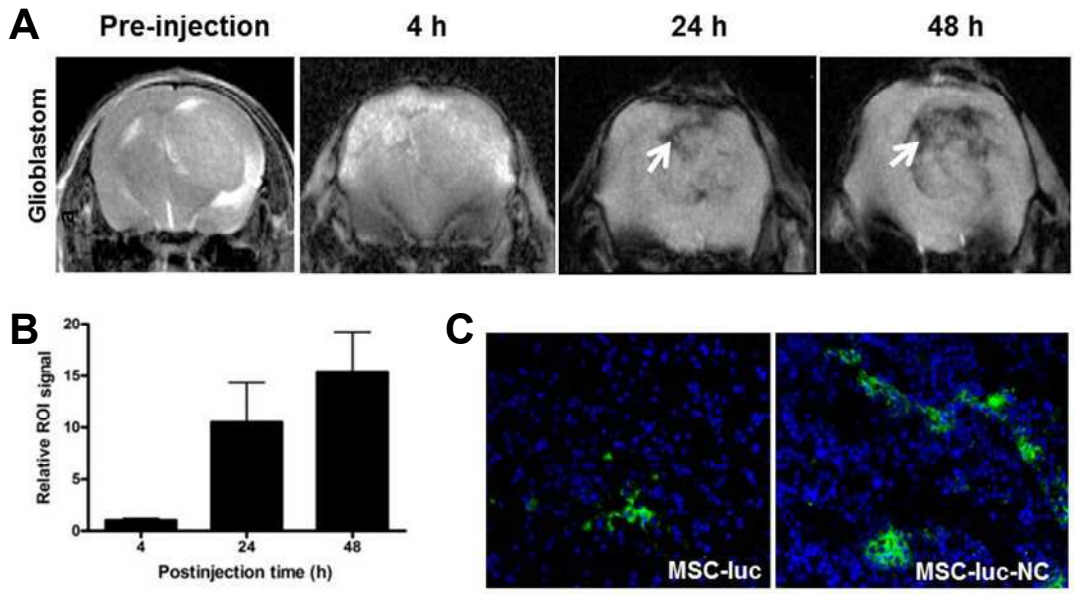

Figure S9. (A) MR images of targeted delivery of HA-$Zn_{0.4}Fe_{2.6}O_4$ NC-labeled MSCs to orthotopic U87MG tumor (arrow). (B) Region of interest (ROI) analysis the relative T_2 signal in the tumor region at different time points after NC-labeled MSCs injection. (C) Immunofluorescence staining of frozen tissue slices confirmed significantly more delivery of NC-labeled MSCs than unlabeled MSCs, both of which express firefly luciferase (fLuc).

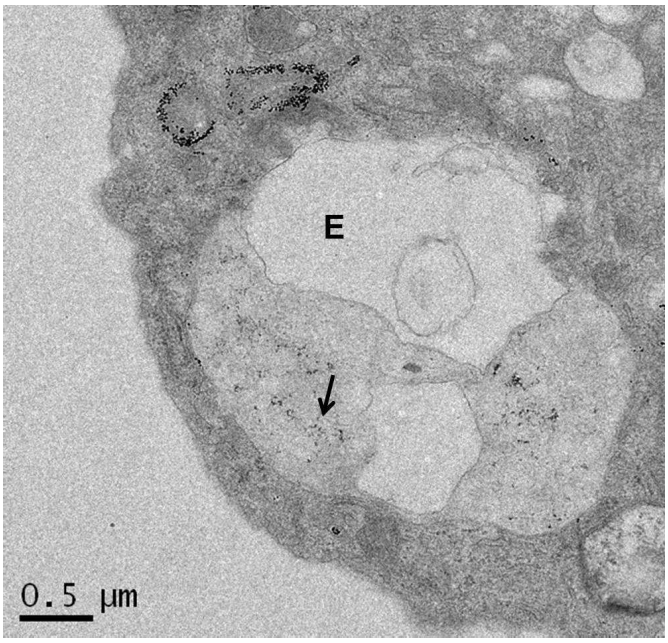

Figure S10. TEM image of NP localization in MSCs. The size of particles was changed from 13 ± 0.5 nm to 7.3 ± 2.6 nm (arrow), which demonstrated the particles were degraded by endosome after 24 h labeling E: endosome.